ChemComm

RSC Publishing

COMMUNICATION

View Article Online
View Journal | View Issue

Cite this: *Chem. Commun.*, 2013, **49**, 1765

Received 17th December 2012, Accepted 10th January 2013

DOI: 10.1039/c3cc39015b

www.rsc.org/chemcomm

Imaging state of charge and its correlation to interaction variation in an $LiMn_{0.75}Fe_{0.25}PO_4$ nanorods–graphene hybrid†

Jigang Zhou,*[ab] Jian Wang,*[a] Yongfeng Hu,[a] Tom Regier,[a] Hailiang Wang,[c] Yuan Yang,[d] Yi Cui[d] and Hongjie Dai[c]

Visualization of the state of charge (SOC) in an $LiMn_{0.75}Fe_{0.25}PO_4$ nanorods–graphene hybrid nanostructure (LMFP–C) is realized by chemical mapping of the Fe valance state using scanning transmission X-ray microscopy (STXM). The LMFP–graphene interaction strength variation studied by C K-edge STXM has been correlated to SOC variation, *i.e.* a stronger interaction was observed for sample regions with a higher SOC in LMFP. Such structure–performance correlation opens new perspectives for a rational design of a better performance olivine cathode for lithium ion batteries.

To make the lithium ion battery another successful revolution in the automobile industry, as it has been in consumer electronics, its high power performance has to be significantly improved, with the primary limitation being with cathode materials.[1] Olivine structured $LiMn_xFe_{1-x}PO_4$ (LMFP) has been elevated into a star as a promising high energy and high power cathode due to its high operation voltage (4.1 V *vs.* 3.5 V in $LiFePO_4$ (LFP)), low cost and low toxicity.[2] The one-dimensional lithium transportation channel in all olivines and the coupling of lithium ions and electron transportation[3] predict an intrinsically low ion and electronic conductivity for all olivines including LMFP solid solution. To overcome this drawback, modifications of LMFP including but not limited to reducing the particle size in the lithium diffusion pathway and surface coating of conducting material like carbon or anchoring nanosized LMFP onto graphene (LMFP–C)[2] have been proved to be effective in improving its power performance. The intimate interaction between LMFP and graphene in LMFP–C *via* a possible P–O–C bonding has been proposed by X-ray absorption near edge structure (XANES) spectroscopy at the C K-edge.[4] This interaction, as has been evidenced by an enhanced C=O absorption peak at 288.5 eV and observed in many carbon nanostructure based hybrid nanostructures,[5–10] not only anchors the nanorods onto the graphene but also modifies its surface chemistry for an enhanced Li^+ diffusion channel, both of which have been proposed to afford the LMFP–C ultrahigh-rate performance in the lithium ion battery.[4] Given the inhomogeneous nature in a hybrid nanostructure, it is plausible to expect a LMFP–graphene interaction strength variation and such variation will result in different electrochemical behaviour during charge and discharge as being assumed in a carbon coated $LiFePO_4$ nanostructure.[3] Studies of the phase change and charge compensation mechanism in LMFP at different states of charge (SOC) during charge (delithiation)–discharge (lithiation) *via in situ* or *ex situ* XRD and hard and soft X-ray absorption spectroscopy (XAS) are a practical approach to understand the involved electrochemistry,[11,12] which has confirmed that Fe is more active than Mn in redox reaction in LMFP.[12] While uniform SOC is the pursuit of a better battery, it is well known of a SOC distribution gradient in battery electrodes primarily due to the polarization effect which results from low materials utilization, localized heating and overcharge or over discharge.[13] A microscopic study of the SOC distribution in a single LMFP–C will allow direct imaging of electrochemical performance difference and correlation of this performance with the structure variation, and thus is of more fundamental importance and should have huge impact on further performance improvement. This work is therefore devoted to provide a deeper understanding of the intimate interaction and its impact on the performance, *i.e.* the structure–performance correlation, which has been proposed in many types of hybrid nanostructure demonstrating super performance enhancement[2,6–8,14–16] but needs a solid experimental proof. Scanning transmission X-ray microscopy (STXM) using a focused beam of the size of ~30 nm provides an excellent combination of microscopic studies and chemical/electronic structure speciation (*via* XANES) of various nanostructures, for instance, studies of the electronic structure and surface interaction of individual CNT or graphene supported catalyst[17] as well as dopant distribution in a single N-doped CNT.[18] This study reports an application of

[a] *Canadian Light Source Inc., Saskatoon, Canada. E-mail: jigang.zhou@lightsource.ca, jian.wang@lightsource.ca*
[b] *Harbin Institute of Technology, Harbin, China*
[c] *Department of Chemistry, Stanford University, USA*
[d] *Department of Materials Science and Engineering, Stanford University, Stanford, CA 94305, USA*

† Electronic supplementary information (ESI) available: Preparation of samples, STXM measurement and data analysis. See DOI: 10.1039/c3cc39015b

STXM in the chemical imaging of redox active Fe valance state distribution (equivalent to SOC distribution) in a partially charged single LMFP–C. Mn L-edge XANES of this sample has proved no oxidation state change at the Mn site (Fig. S2, ESI†). The Fe valance state distribution is then correlated to the interaction strength extracted by the C K-edge STXM XANES from the same LMFP–C hybrid nanostructure. LMFP–C was made by a two-step solution method. The preparation details have been reported earlier[2] and are briefly described in the ESI.† Delithiation of LMFP–C was achieved by charging a coin cell in which the LMFP–C hybrid nanostructure was the cathode active material. LMFP–C charged to the end of the first and the second plateaus (Fig. S1, ESI†) was recovered from the disassembled coin cell and denoted as partially charged and fully charged, respectively. The STXM was performed on the SM beamline at the Canadian Light Source (CLS). The STXM experimental details have been described elsewhere.[17,18] In short, the monochromatic X-ray beam is focused by a Fresnel zone plate lens to an ~30 nm spot on the sample. The sample is raster-scanned with synchronized detection of transmitted X-rays to generate images. Chemical imaging and XANES spectra are obtained using image sequence (stack) scans over a range of photon energies. STXM data were analysed by aXis2000. Chemical component maps for Fe valance state distribution (SOC distribution) in the partially charged LMFP–C were obtained by fitting the Fe L-edge stack with linear reference spectra of pristine LMFP (Fe^{2+}) and fully charged LMFP (Fe^{3+}). More details of experimental and data analysis are given in the ESI.†

The STXM generated chemical maps are shown in Fig. 1a (Fe^{2+}) and Fig. 1b (Fe^{3+}). The grey scales in the figures represent the absolute thickness distribution of LMFP and MFP in this hybrid nanostructure. It is obvious from the chemical mapping that there is still a significant amount of Fe^{2+} in the partially charged LMFP–C. This agrees well with the soft X-ray XAS of LMFP,[12] which shows that charging LMFP to the first plateau cannot convert all Fe^{2+} to Fe^{3+}. In the colour composite map in Fig. 1c it can be observed that Fe^{2+} and Fe^{3+} appeared to enrich in distinct certain regions where a boxed region only has Fe^{2+} and a circulated region is Fe^{3+} dominated. This clearly presents the SOC variation in this single LMFP–C. Fig. 1c also shows that fully charged species (Fe^{3+}) resembles more the rod shape than the Fe^{2+} does, which highlights the importance of morphology in the performance,[2] which is worthy of a further study by STEM. Both observations raise the possibility that the SOC variation is more distinct among than within individual rods although 30 nm spatial resolution is not enough to probe very small nanorods. The SOC variation between regions in this LMFP–C could be aligned to the domino-cascade delithiation model,[3] which predicts the coexistence of fully charged (Fe^{3+}) and fully lithiated (Fe^{2+}) nanostructures (100 nm in diameter) in a partially charged $LiFePO_4$. The domino-cascade delithiation was limited by the nucleation process in nanostructured $LiFePO_4$ which is in contrast to a diffusion limited delithiation in larger sized $LiFePO_4$, where a SOC difference occurs inside a particle.[19] The LMFP nanorods in this study are only ~30 nm in diameter and 50–100 nm in length with the lithium

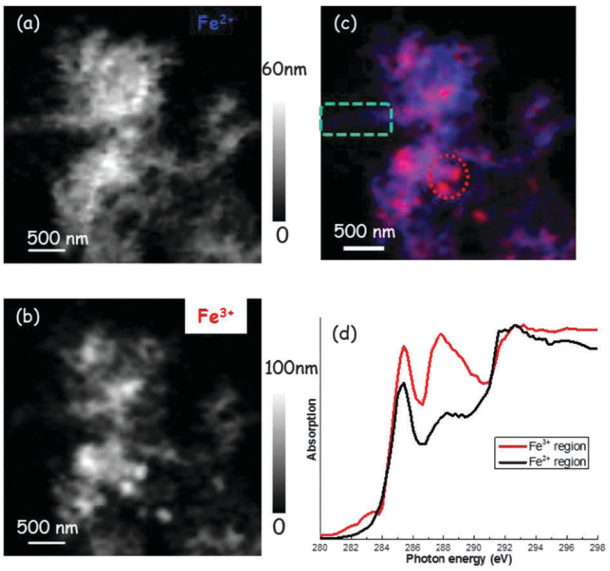

Fig. 1 STXM chemical maps of partially charged LMFP–C for visualizing the Fe valance distribution: (a) Fe^{2+} and (b) Fe^{3+}, grey scale represents the thickness in nm; (c) the colour composite map of Fe^{2+} and Fe^{3+} (blue: Fe^{2+}, red: Fe^{3+}). The selected Fe^{2+} and Fe^{3+} regions are highlighted by the rectangular and circular box, respectively; (d) C K-edge XANES from the selected areas as displayed in 1(c).

transportation channel [010] along the radius.[2] It was assumed that a better carbon coating, *i.e.* a good electronic conductivity, facilitates the charge–discharge process of LMFP. Here we provide experimental support to this hypothesis by correlating the delithiation (*via* SOC mapping) with the carbon coating (*via* C K-edge XANES). We selected an Fe^{2+} region and an Fe^{3+} region as shown in the enclosures in Fig. 1c to study the carbon structure difference by STXM at the C K-edge. To ensure an identical sample region in different edges the Fe and C edge image stacks were appended together to form a whole stack, and then aligned. The obtained C K-edge XANES from the Fe^{2+} rich (low SOC) and from the Fe^{3+} rich (high SOC) region are displayed in Fig. 1d. Due to the dipole selection rules, C K-edge XANES is dominated by the transitions from C 1s electrons to unoccupied C 2p states. It features two main peaks at ~285 and ~293 eV attributable to C 1s to graphitic C–C π^* and C–C σ^* transitions, respectively. The existence of the π^* peak and the resolved double peaks in the σ^* region confirm the graphitic framework in the imaged hybrid nanostructures. The dominant graphitic feature also rules out the possible contribution from PVdF as a binder used in forming the electrode since it doesn't have any graphitic feature. Along with those common graphite features, there is a peak at ~288 eV which is consistent with transitions to C–O states and most likely of P–O–C in this sample to link LMFP to graphene by a covalent bonding.[4] The intensity shall be an indicator of the interaction strength in terms of the amount of functionalization between LMFP and graphene. Very interestingly, this feature is significantly enhanced in the Fe^{3+} rich region, which means a stronger interaction in the Fe^{3+} rich region than that in the Fe^{2+} rich region. C K-edge STXM was fitted by the spectra in Fig. 1d and the colour composite map can be generally correlated to Fe^{3+} and Fe^{2+} distribution in Fig. 1c (Fig. S3, ESI†). The nature of a stronger

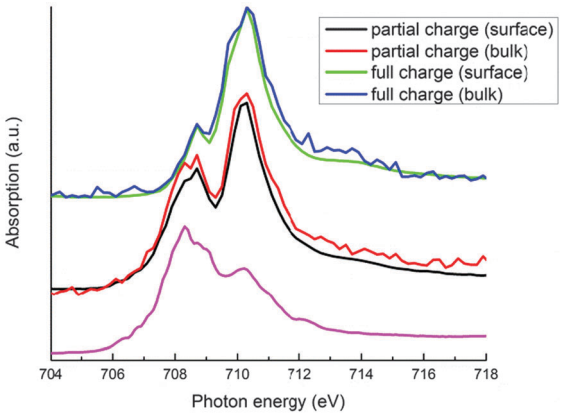

Fig. 2 Fe L-edge XANES of LMFP–C at various SOC stages, partially charged (middle ones using TEY and IPFY), and fully charged (top two using TEY and IPFY) along with the pristine one (bottom one, 100% Fe^{2+}).

interaction could be stronger covalent bonding with the same amount of bonding sites or more bonding sites between single LMFP and graphene substrate. This clearly correlates the structural variation among single LMFP–C to its performance difference, *i.e.* stronger interaction between components affords a higher SOC. This observation verifies our assumption of the significance of the intimate bonding in hybrid nanostructures.[6,8] This also provides the first experimental evidence of the importance of carbon coating in delithiation performance as proposed in the domino-cascade model,[3] though further study is needed to unveil the relevance of electron conduction to the strong interaction.

To further verify the above microscopic result that the SOC varies among LMFP nanorods than within nanorods, we conducted macroscopic XANES spectroscopy of partially and fully charged electrodes made of LMFP–C at the Fe L-edge by simultaneously obtaining the inverse partial fluorescence yield (IPFY)[20] signal for the bulk with a probing depth at about 100 nm and the total electron yield (TEY) for the surface of the sample with a probing depth of few nm. Electronic transitions from the Fe $2p_{3/2}$ level to the unoccupied 3d states are the origin of the Fe L_3 edge XANES. The associated spectra are split by a combination of crystal filed splitting, multiplet effect and ligand hybridization. The spectral features can unravel rich electronic and structural information[21] and can be used to determine the valance state of Fe in LMFP as in the previous STXM section. In Fig. 2, we show the Fe L_3-edge XANES of LMFP (partially charged and fully charged) using TEY and IPFY along with the reference spectrum of the pristine LMFP. Clearly, charging (delithiation) does change the XANES in terms of the shape of the spectrum in that the pristine one corresponds to Fe^{2+} and the fully charged one to Fe^{3+}, while the partially charged one represents a mixture of Fe^{3+} and Fe^{2+}. This is fully consistent with our STXM observation and that has also been reported in the literature.[12] Interestingly, Fe valance of the surface and bulk in the partially charged LMFP doesn't show significant difference, as well as in the fully charged LMFP.

In summary, the chemical mapping of Fe valance state variation in a single LMFP nanorods covered graphene sheet after being partially charged has been obtained by STXM with a spatial resolution of 30 nm. Variation in Fe valance (Fe^{2+} *versus* Fe^{3+}) distribution reflects the state of charge variation within this single hybrid nanostructure. SOC variation within the single LMFP–C hybrid nanostructure could be explained by a domino-cascade delithiation process in this hybrid nanostructure, which will result in separately charged and non-charged LMFPs. This variation corresponds to electrochemical dynamic difference between LMFPs. This point has been further verified by the collective Fe L-edge XANES which shows identical spectroscopy features from the top few nanometers and the bulk of the nanorods of a partially charged LMFP electrode. More importantly, this SOC difference among single LMFP–C hybrid nanostructures has been correlated to the LMFP–graphene interaction difference as being extracted from the C K-edge STXM, *i.e.* a stronger interaction between LMFP and graphene corresponds to a higher SOC. The results support our assumption of the crucial role of the intimate interaction of the hybrid nanostructure in achieving super performance and will advance our understanding of the intrinsic relation between structure and performance of not only LMFP–graphene in this case but can also be extended to many different nano-hybrids.

CLS is supported by NSERC, NRC, CIHR and the University of Saskatchewan.

Notes and References

1 B. Kang and G. Ceder, *Nature*, 2009, **458**, 190–193.
2 H. L. Wang, Y. Yang and Y. Y. Liang, *et al*, *Angew. Chem., Int. Ed.*, 2011, **50**, 7364–7368.
3 C. Delmas and M. Maccario, *et al*, *Nat. Mater.*, 2008, **7**, 665–671.
4 J. G. Zhou, J. Wang and L. Zuin, *et al*, *Phys. Chem. Chem. Phys.*, 2012, **14**, 9578–9581.
5 J. G. Zhou, *et al*, *J. Mater. Chem.*, 2011, **21**, 14622–14630.
6 Y. Liang, Y. Li and H. Wang, *et al*, *Nat. Mater.*, 2011, **10**, 780–786.
7 Y. Liang and H. Wang, *et al*, *J. Am. Chem. Soc.*, 2012, **134**, 3517–3523.
8 H. L. Wang and Y. Y. Liang, *et al*, *Nat. Commun.*, 2012, 3.
9 J. G. Zhou, H. T. Fang and Y. F. Hu, *et al*, *J. Phys. Chem. C*, 2009, **113**, 10747–10750.
10 J. G. Zhou and H. T. Fang, *et al*, *J. Phys. Chem. C*, 2009, **113**, 6114–6117.
11 K. W. Nam, W. S. Yoon, K. Zaghib, K. Y. Chung and X. Q. Yang, *Electrochem. Commun.*, 2009, **11**, 2023–2026.
12 H. M. Hollmark, T. Gustafsson, K. Edstrom and L. C. Duda, *Phys. Chem. Chem. Phys.*, 2011, **13**, 20215–20222.
13 J. Liu, M. Kunz, K. Chen, N. Tamura and T. J. Richardson, *J. Phys. Chem. Lett.*, 2010, **1**, 2120–2123.
14 Y. Y. Liang, H. L. Wang, H. S. Casalongue, Z. Chen and H. J. Dai, *Nano Res.*, 2010, **3**, 701–705.
15 H. L. Wang, H. S. Casalongue, Y. Y. Liang and H. J. Dai, *J. Am. Chem. Soc.*, 2010, **132**, 7472–7477.
16 H. L. Wang, L. F. Cui and Y. A. Yang, *et al*, *J. Am. Chem. Soc.*, 2010, **132**, 13978–13980.
17 J. G. Zhou, J. Wang, H. T. Fang and C. X. Wu, *et al*, *Chem. Commun.*, 2010, **46**, 2778–2780.
18 J. G. Zhou, J. A. Wang, H. Liu, M. N. Banis, X. L. Sun and T. K. Sham, *J. Phys. Chem. Lett.*, 2010, **1**, 1709–1713.
19 W. Sigle, R. Amin, K. Weichert, P. A. van Aken and J. Maier, *Electrochem. Solid–State Lett.*, 2009, **12**, A151–A154.
20 A. J. Achkar, T. Z. Regier, H. Wadati, Y. J. Kim, H. Zhang and D. G. Hawthorn, *Phys. Rev. B: Condens. Matter Mater. Phys.*, 2011, **83**, 081106.
21 X. S. Liu, J. Liu and R. M. Qiao, *et al*, *J. Am. Chem. Soc.*, 2012, **134**, 13708–13715.